Al-imad Journal of Humanities and Applied Sciences (AJHAS)
مجلة العماد للعلوم الإنسانية والتطبيقية
ISSN: 3106-0323
Volume 2 – Issue 1 – 2026
Pages 352-372

Gas Geochemistry of the Ordovician–Carboniferous Sediments in Well A1-NC175, Ghadames Basin, NW Libya

Osama Rahil Shaltami[1] , Abdullah Yousuf Altarhouni [2], Mustafa A. Ben Hkoma [3]
[1]Department of Earth Sciences, Faculty of Science, Benghazi University, Libya
[1,3] Libyan Centre for Sustainable Development Researches
[2] Sirte Oil Company, Libya
*Corresponding: m_hkoma2017@yahoo.com

الجيوكيمياء الغازية للرواسب الأوردوفيسية-الكربونية في البئر *A1-NC175* ، حوض غدامس، شمال غرب ليبيا

أسامة رحيل الشلطامي[1]، عبدالله يوسف الترهوني [2]، مصطفى بن حكومة[3]
[1]قسم علوم الأرض، كلية العلوم، جامعة بنغازي، ليبيا
[3،1] المركز الليبي لأبحاث التنمية المستدامة
[2] شركة سرت للنفط ، ليبيا

Received: 10-01-2026; Accepted: 12-02-2026; Published: 23-03-2026

Abstract:
The authors evaluated the geochemical characteristics of source rock and natural gas of the Ordovician–Carboniferous strata in well A1-NC175, Ghadames Basin, NW Libya. In terms of the source rock geochemistry, the organic richness ranged from poor to good. The predominant kerogen was of type III and IV. There were three levels of thermal maturity: early, peak, and late. The shales mainly contained indigenous hydrocarbons. The shales may be regarded as oil and/or gas sources. The shales are not considered a potential reservoir for extracting unconventional hydrocarbons. In terms of the gas geochemistry, thermogenic gases predominated in the samples. The gasses were wet in nature.

Keywords: Source Rock Geochemistry, Gas Geochemistry, Ordovician–Carboniferous Sediments, Ghadames Basin, Libya.

الملخص
قام الباحثون بتقييم الخصائص الجيوكيميائية للصخور المصدرية والغاز الطبيعي في طبقات العصرين الأوردوفيسي والكربوني في البئر A1-NC175، حوض غدامس، شمال غرب ليبيا. وفيما يخص الخصائص الجيوكيميائية للصخور المصدرية، تراوحت نسبة المواد العضوية فيها من ضعيفة إلى جيدة. وكان الكيروجين السائد من النوعين الثالث والرابع. وظهرت ثلاثة مستويات من النضج الحراري: مبكر، وذروة، ومتأخر. واحتوت الصخور الطينية بشكل رئيسي على هيدروكربونات محلية. ويمكن اعتبارها مصادر للنفط و/أو الغاز، إلا أنها لا تُعدّ خزاناً محتملاً لاستخراج الهيدروكربونات غير التقليدية. أما فيما يخص الخصائص الجيوكيميائية للغاز، فقد سادت الغازات الحرارية في العينات، وكانت هذه الغازات رطبة.
الكلمات المفتاحية: الخصائص الجيوكيميائية للصخور المصدرية، الخصائص الجيوكيميائية للغاز، رواسب العصرين الأوردوفيسي والكربوني، حوض غدامس، ليبيا.

1. Introduction

 Copyright: © 2026 by the authors. Submitted for possible open access publication under the terms and conditions of the Creative Commons Attribution (CC BY) license (https://creativecommons.org/licenses/by/4.0/).

One of Libya's sedimentary basins is the Ghadames Basin. It is 350,000 km^2 in size. The center of the basin is located in Algeria. The eastern portion is characterized by the Libyan section, which ascends to the Tripoli–Tibisti Arch and encompasses the Zamzam Depression that extends to the east (Hallett and Clark-Lowes, 2016). There are 21,000 ft and 18,000 ft of basin-fill in Algeria and Libya, respectively. The Hoggar Massif in Algeria and the Qarqaf Arch in Libya to the south, the Amguid-El Biod Uplift in Algeria to the west, and the Dahar–Nafusah Arch to the north form the basin's borders. The basin extends eastward beneath the western part of the Sirte Basin. The time stratigraphic chart of west Libya is displayed in Fig. 1.

Determining the geochemical characteristics of source rock and natural gas of the Mamuniyat (Late Ordovician), Tanezzuft (Early Silurian), Tadrart (Early Devonian), Awainat Wanin (Late Devonian), Marar (Early Carboniferous), Assedjefar (Late Carboniferous), and Dembaba (Late Carboniferous) formations in well A1-NC175, Ghadames Basin, NW Libya (Fig. 2), is the goal of this study.

 Copyright: © 2026 by the authors. Submitted for possible open access publication under the terms and conditions of the Creative Commons Attribution (CC BY) license (https://creativecommons.org/licenses/by/4.0/).

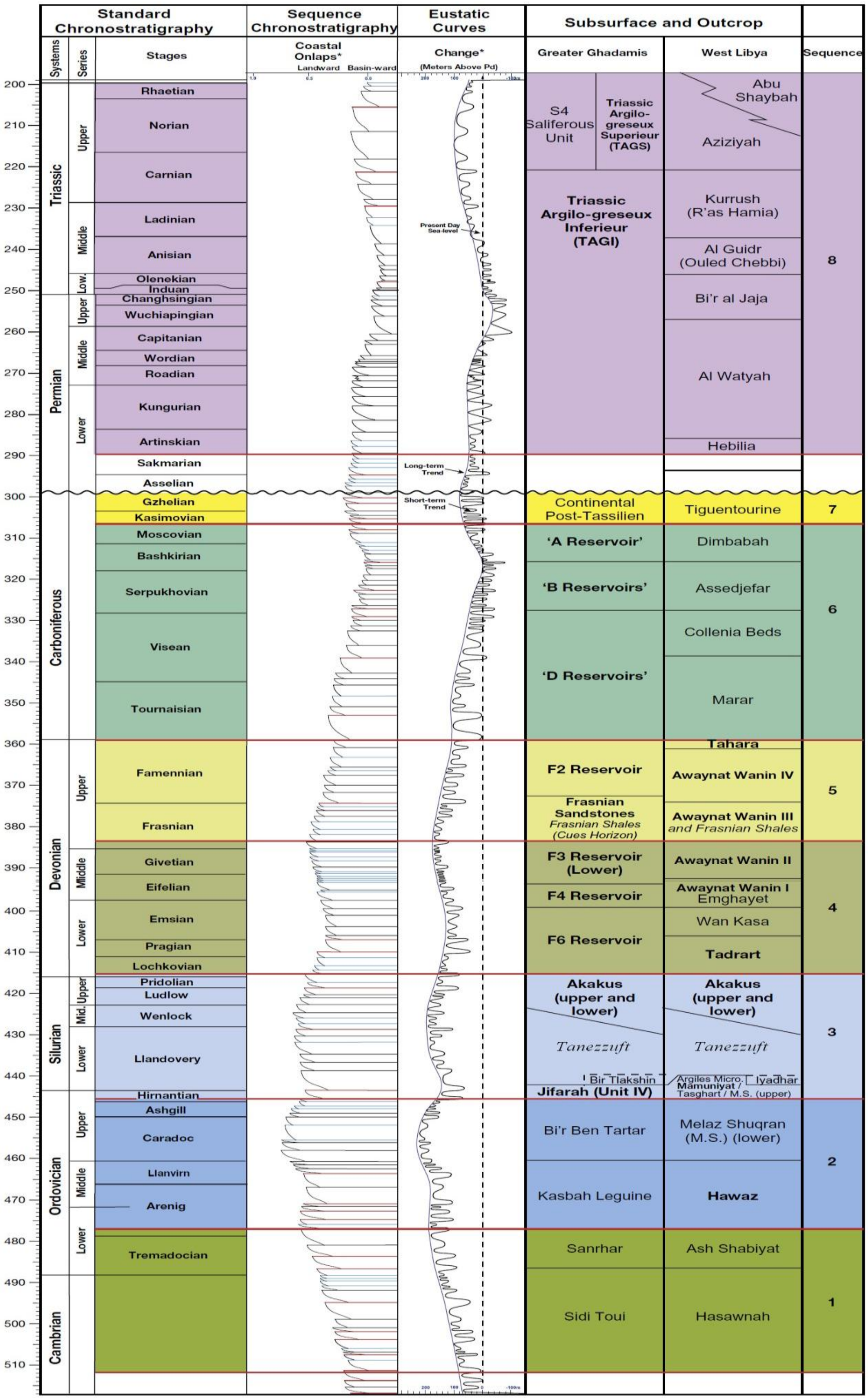

Fig. 1: Time stratigraphic chart of west Libya (bold lettering indicates petroleum reservoir; italic script indicates source rock) (after Carr, 2002; Haq and Schutter, 2008; Galeazzi et al., 2010).

 Copyright: © 2026 by the authors. Submitted for possible open access publication under the terms and conditions of the Creative Commons Attribution (CC BY) license (https://creativecommons.org/licenses/by/4.0/).

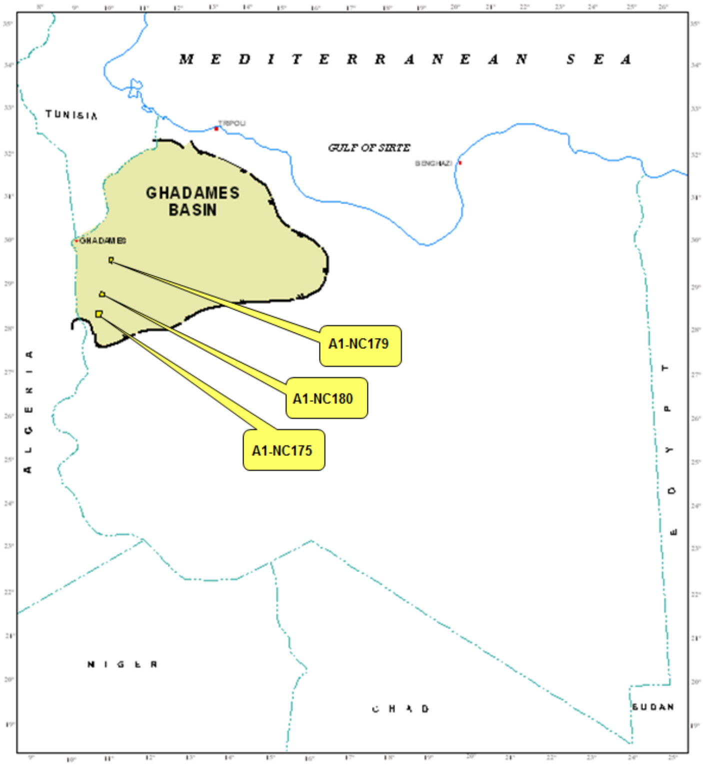

Fig. 2: Location map of well A1-NC175.

The lower and upper parts of the Mamuniyat and Tadrart formations were deposited in different environments (fluvial and marine, respectively, McDougall *et al.*, 2005). The definite environment of the Awainat Wanin, Marar, and Assedjefar formations is the deltaic setting (Vos, 1981; Aziz, 2000; Shalbak, 2015), while the Tanezzuft and Dembaba formations record deposition in a marine environment (Hallett, 2002). The studied formations have been the subject of numerous geochemical studies (e.g., Lüning *et al.*, 2000; Hrouda, 2004; Fello *et al.*, 2006; Hall *et al.*, 2010; Belaid *et al.*, 2010; Hodairi and Philp, 2011; Elkelani, 2014; EIA, 2015; Abohajar *et al.*, 2015; Meinhold *et al.*, 2016, 2021; El Diasty *et al.*, 2017; Aboglila *et al.*, 2018, 2020; Musa, 2019; Albaghdady *et al.*, 2020, 2024; Shaltami *et al.*, 2021, 2025; Albriki *et al.*, 2022, 2024; Muhammed, 2024; Shaltami, 2024; Edegbai, and Ogbe, 2024; Boshnyif *et al.*, 2025).

2. Methodology

The National Oil Corporation (NOC), Libya, supplied the chemical data used in this study. The following is the work plan:

(1) Chemical analysis of 11 cutting shale samples (at depths of 3870 to 8250 ft) from the studied formations was carried out using a Rock-Eval pyrolysis.

 Copyright: © 2026 by the authors. Submitted for possible open access publication under the terms and conditions of the Creative Commons Attribution (CC BY) license (https://creativecommons.org/licenses/by/4.0/).

(3) The gas types of 30 samples (at depths of 2750 to 7750 ft) was determined using a gas chromatography (GC).

(4) Isotope ratio mass spectrometry (IRMS) was used to identify the stable carbon isotopes of 30 samples (at depths of 2750 to 7750 ft).

Table 1 presents the abbreviations and equations for the parameters used in this investigation. The parameters' interpretation is revealed in Table 2.

3. Results and Discussion

3.1. Source Rock Geochemistry

Eleven samples from well A1-NC175 underwent Rock-Eval pyrolysis (Table 3) to assess the geochemical characteristics of source rock. The discrimination diagrams (Figs. 3 and 4) demonstrated three levels of organic richness in the examined shale: poor, fair, and good. The Ordovician–Carboniferous shales is dominated by type III and IV kerogen as shown in the diagrams (Figs. 5 and 6). Furthermore, the diagrams indicate three levels of thermal maturity: early, peak, and late (Figs. 7 and 8). Indigenous hydrocarbons predominate in the shales, according to the plot of TOC versus S1 (Fig. 9). The shales can be considered sources of oil and/or gas, as illustrated by the diagram of TOC versus HI (Fig. 10). The shales have OSI values below 100 (Fig. 11), which suggests that the oil is either retained or sorbed within the rock matrix or is not readily producible. This indicates a higher risk for shale oil exploration because these values typically indicate a lack of high-saturation, producible oil.

3.2. Gas Geochemistry

The natural gas types in the Ordovician–Carboniferous sediments are shown in Table 4. Table 5 displays the isotopic composition of the studied gases. The strata are dominated by thermogenic gas, as shown by the discrimination diagrams (Figs. 12 and 13). It should be noted that $\delta^{13}C_{CO2}$ was only identified in four samples from the Marar and Awainat Wanin formations; hence the origin of CO_2 was only assessed in these samples. The diagram of wetness versus $\delta^{13}C2$ (Fig. 14) shows that wet gas is dominant in the strata. The values of C1/(C2+C3) and $C1/\Sigma C_n$ (0.08-31.72 and 0.02-9.02, respectively) supports this assumption.

4. Conclusions

Geochemical study was performed on the source rock and natural gas of the Ordovician–Carboniferous strata in well A1-NC175, Ghadames Basin, NW Libya. There are eight conclusions:

 Copyright: © 2026 by the authors. Submitted for possible open access publication under the terms and conditions of the Creative Commons Attribution (CC BY) license (https://creativecommons.org/licenses/by/4.0/).

(1) The shales exhibited diverse levels of organic matter richness (from poor to good).

(2) The shales contained kerogen of type III and IV.

(3) The shales revealed three stages of thermal maturity: early, peak, and late.

Table 1: Abbreviations and equations of the parameters used in this investigation

Parameter	Abbreviation and equation
Total organic carbon (wt%)	TOC
Quantity of free hydrocarbons (mg/g)	S1
Quantity of generated hydrocarbons (mg/g)	S2
Quantity of CO_2 generated during pyrolysis (mg/g)	S3
Temperature at which maximum rate of generation of hydrocarbons occurs (°C)	T_{max}
Hydrogen index (mg/g)	HI = S2/TOC × 100
Oxygen index (mg/g)	OI = S3/TOC × 100
Oil saturation index (mg/g)	OSI = S1/TOC × 100
Production index	PI = S1/(S1+S2)
Pyrolyzable carbon index (mg/g)	PCI = 0.83(S1+S2)
Spore color index	SCI
Vitrinite reflectance	$R_0 = 0.018 \times T_{max} - 7.16$
Billion cubic feet	Bcf
Billion barrels	B bbl
Million barrels	MM bbl
Trillion cubic feet	Tcf
Gas in-place	GIP
Oil in-place	OIP
Methane	C1
Ethane	C2
Propane	C3
Isobutane	i-C4
n-butane	n-C4
Isopentane	i-C5
n-pentane	n-C5
Hexane and heavier hydrocarbons (e.g., heptane, octane, nonane)	C6+
Stable carbon isotope of methane	$\delta^{13}C1$
Stable carbon isotope of ethane	$\delta^{13}C2$
Stable carbon isotope of propane	$\delta^{13}C3$
Stable carbon isotope of n-butane	$\delta^{13}nC4$
Stable carbon isotope of n-pentane	$\delta^{13}nC5$
Stable carbon isotope of carbon dioxide	$\delta^{13}C_{CO2}$
Wetness	Wetness = ((C2+C3+C4+C5)/ (C1+C2+C3+C4+C5))*100

(4) The shales were dominated by indigenous hydrocarbons.

(5) The shales are sources of oil and/or gas.

(6) Unconventional hydrocarbons cannot be economically extracted from the shales.

(7) The strata were characterized by the presence of thermogenic gasses.

(8) The predominant gases in the strata were of the wet type.

 | Copyright: © 2026 by the authors. Submitted for possible open access publication under the terms and conditions of the Creative Commons Attribution (CC BY) license (https://creativecommons.org/licenses/by/4.0/).

Table 2: Interpretation of the parameters

Objective	Parameter	Values	Interpretation	Reference
Organic richness	TOC (%)	0–0.5	Poor	Peters and Cassa (1994)
		0.5–1	Fair	
		1–2	Good	
		2–4	Very good	
		>4	Excellent	
	S1	0–0.5	Poor	
		0.5–1	Fair	
		1–2	Good	
		2–4	Very good	
		>4	Excellent	
	S2	0–2.5	Poor	
		2.5–5	Fair	
		5–10	Good	
		10–20	Very good	
		>20	Excellent	
Kerogen type	HI (mg/g)	<50	Type IV	
		50–200	Type III	
		200–300	Type II-III	
		300–600	Type II	
		>600	Type I	
	S2/S3	<1	Type IV	
		1–5	Type III	
		5–10	Type II-III	
		10–15	Type II	
		>15	Type I	
	PCI (mg/g)	<15	Type III	Reed and Ewan (1986)
		40–50	Type II	
		≥75	Type I	
Thermal maturity	T_{max} (^{o}C)	<435	Immature	Peters and Cassa (1994)
		435–445	Early mature	
		445–450	Peak mature	
		450–470	Late mature	
		>470	Postmature	
	R_0	0.2–0.6	Immature	
		0.6–0.65	Early mature	
		0.65–0.9	Peak mature	
		0.9–1.35	Late mature	
		>1.35	Postmature	
	PI	<0.1	Immature	
		0.1–0.15	Early mature	
		0.25–0.4	Peak mature	
		>0.4	Late mature	
		-	Postmature	
Thermal maturity	C1/(C2+C3)	<50	Wet gas	Whiticar (1999)
		>50	Dry gas	
	C1/ΣCn	<97	Wet gas	Tissot and Welte (1984)
		>97	Dry gas	
	Wetness	>8%	Pre-rollover zone	Feng *et al.* (2016)
		>0.8% and <8%	Rollover zone	
		<0.8%	Post-rollover zone	
Indigeneity	S1/TOC	<1.5	Indigenous hydrocarbons	Hunt (1996)
		>1.5	Nonindigenous hydrocarbons	
Unconventional hydrocarbons	OSI	<100	Unsuitable potential	Tian *et al.* (2024)
		>100	Suitable potential	

Table 3: Rock Eval pyrolysis data of the Ordovician–Carboniferous sediments in well A1-NC175

 Copyright: © 2026 by the authors. Submitted for possible open access publication under the terms and conditions of the Creative Commons Attribution (CC BY) license (https://creativecommons.org/licenses/by/4.0/).

Formation	Lithology	Depth (ft)	TOC	S1	S2	S3	OI
Marar	Shale	3870	1.24	0.06	0.67	0.43	35
		4770	0.6	0.06	0.31	0.47	78
Awainat Wanin	Shale	6150	1.52	0.53	2.11	0.59	39
		6240	1.15	0.37	1.51	0.86	75
		6410	1	0.25	1.12	0.48	48
		6480	1.1	0.3	1.32	0.43	39
		6720	0.88	0.23	0.91	0.44	50
		6900	0.89	0.24	1.09	0.41	46
Tanezzuft	Shale	7560	0.4	0.07	0.27	0.39	98
		7800	0.95	0.18	0.31	0.56	59
Mamuniyat	Shale	8250	0.81	0.3	0.65	0.5	62

Table 3: Continued

Formation	Lithology	Depth (ft)	HI	T_{max}	R_0	PI	OSI	PCI
Marar	Shale	3870	54	440	0.76	0.08	4.84	0.61
		4770	52	436	0.69	0.16	10	0.31
Awainat Wanin	Shale	6150	139	449	0.92	0.2	34.87	2.19
		6240	131	447	0.89	0.2	32.17	1.56
		6410	111	449	0.92	0.18	25	1.14
		6480	120	450	0.94	0.19	27.27	1.34
		6720	103	450	0.94	0.2	26.14	0.95
		6900	122	448	0.9	0.18	26.97	1.1
Tanezzuft	Shale	7560	68	452	0.98	0.21	17.5	0.28
		7800	33	455	1	0.37	18.95	0.41
Mamuniyat	Shale	8250	80	442	0.8	0.32	37.04	0.79

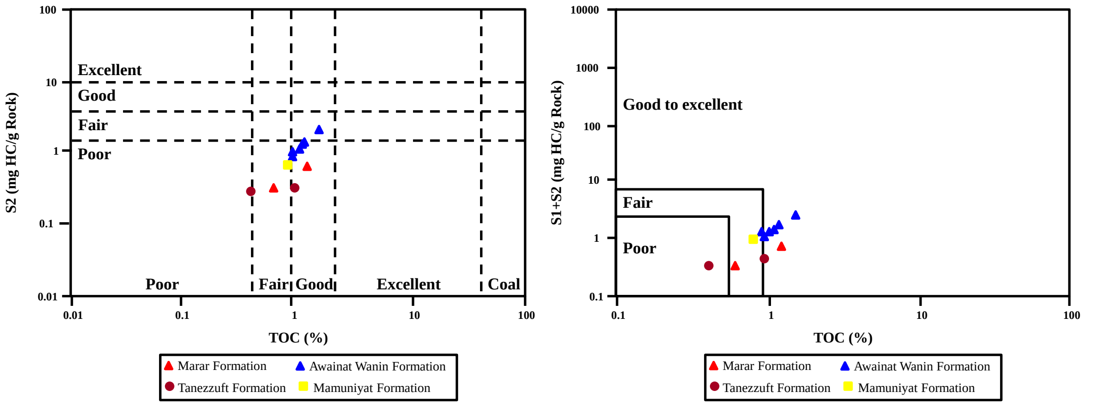

Fig. 3: Binary plots (TOC vs. S2 (fields after Dembicki, 2009) and TOC vs. S1+S2 (fields after Tissot and Welte, 1984)) showing the organic richness of the Ordovician–Carboniferous shales in well A1-NC175.

 Copyright: © 2026 by the authors. Submitted for possible open access publication under the terms and conditions of the Creative Commons Attribution (CC BY) license (https://creativecommons.org/licenses/by/4.0/).

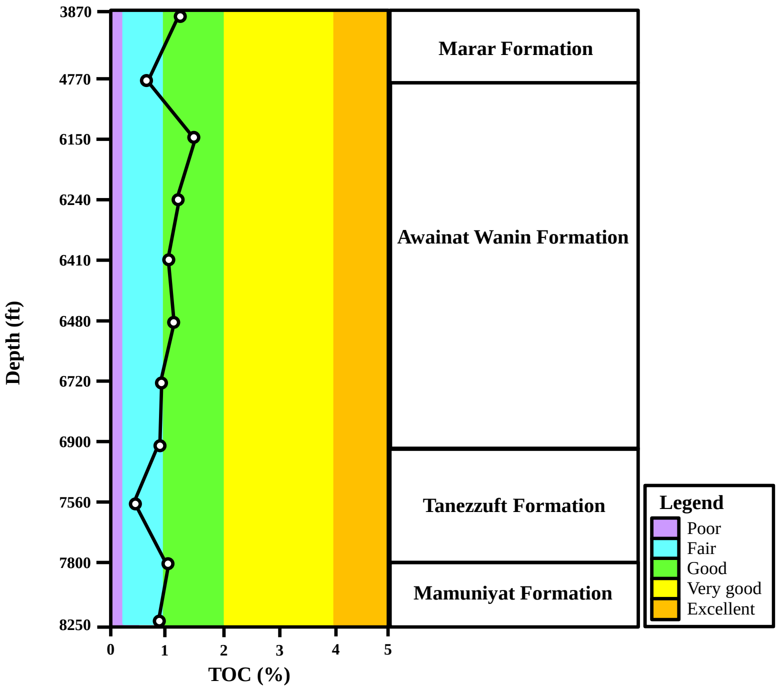

Fig. 4: Binary plot of TOC vs. depth showing the organic richness of the Ordovician–Carboniferous shales in well A1-NC175 (fields after Peters and Cassa, 1994).

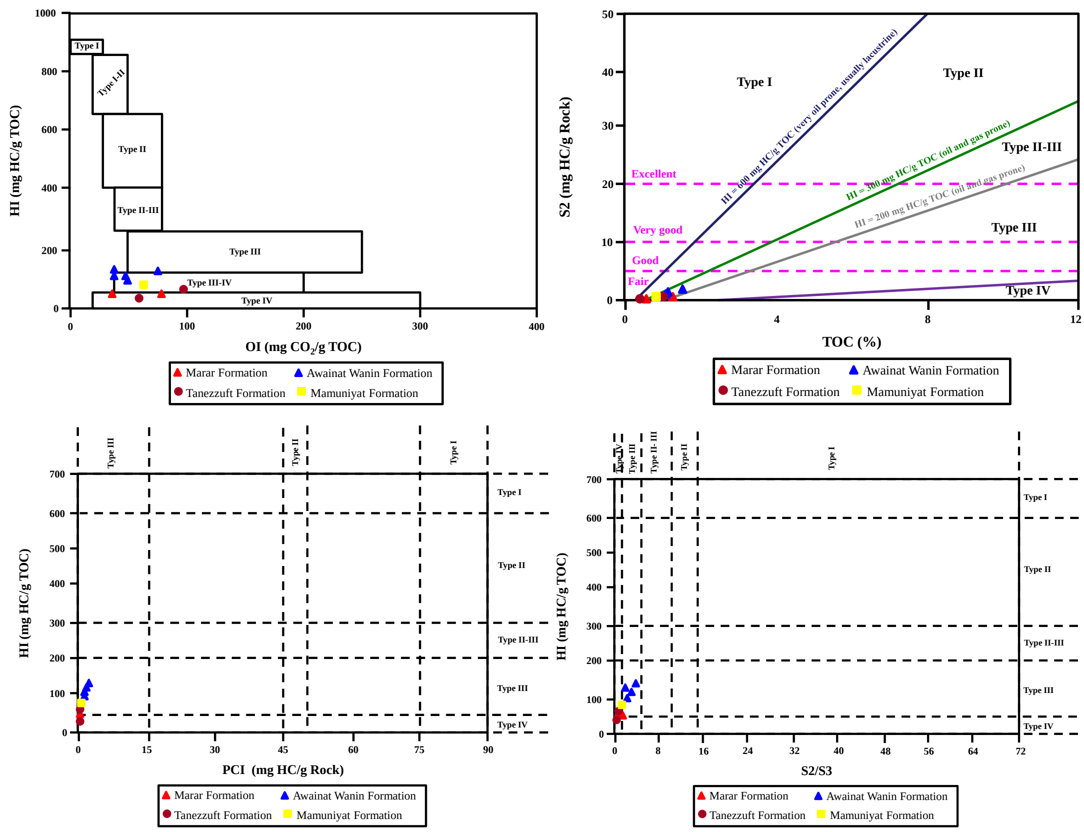

Fig. 5: Binary plots of (OI vs. HI (fields after Jones, 1987), TOC vs. S2 (fields after Longford and Blanc-Valleron, 1990), PCI vs. HI (fields after Reed and Ewan, 1986; Peters and Cassa,

 Copyright: © 2026 by the authors. Submitted for possible open access publication under the terms and conditions of the Creative Commons Attribution (CC BY) license (https://creativecommons.org/licenses/by/4.0/).

1994), and S2/S3 vs. HI (fields after Peters and Cassa, 1994)) showing the kerogen type of the Ordovician–Carboniferous shales in well A1-NC175.

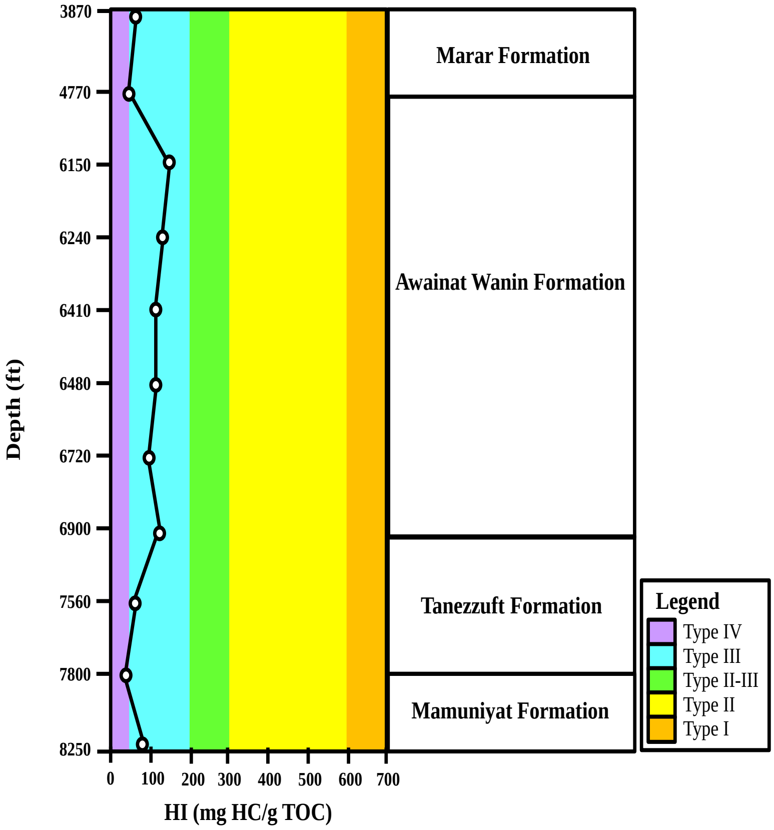

Fig. 6: Binary plot of HI vs. depth showing the kerogen type of the Ordovician–Carboniferous shales in well A1-NC175 (fields after Peters and Cassa, 1994).

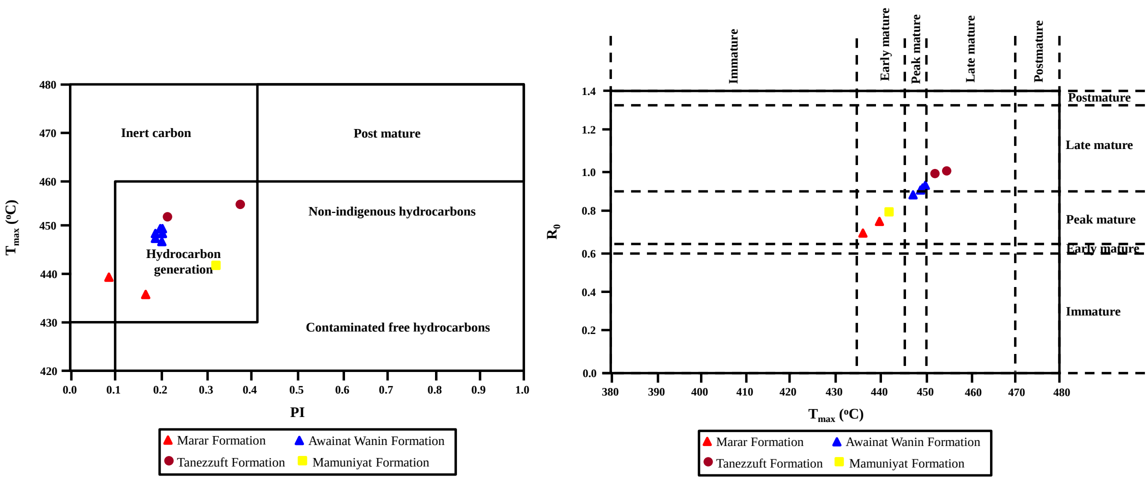

 | Copyright: © 2026 by the authors. Submitted for possible open access publication under the terms and conditions of the Creative Commons Attribution (CC BY) license (https://creativecommons.org/licenses/by/4.0/).

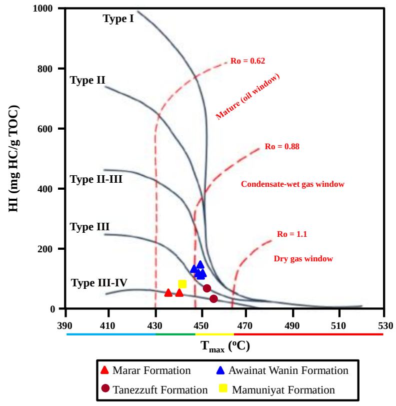

Fig. 7: Binary plots (PI vs. T_{max} (fields after Tissot and Welte, 1984), T_{max} vs. R_0 (fields after Peters and Cassa, 1994), and T_{max} vs. HI (fields after Hall et al., 2016)) showing the thermal maturity of organic matter in the Ordovician–Carboniferous shales in well A1-NC175.

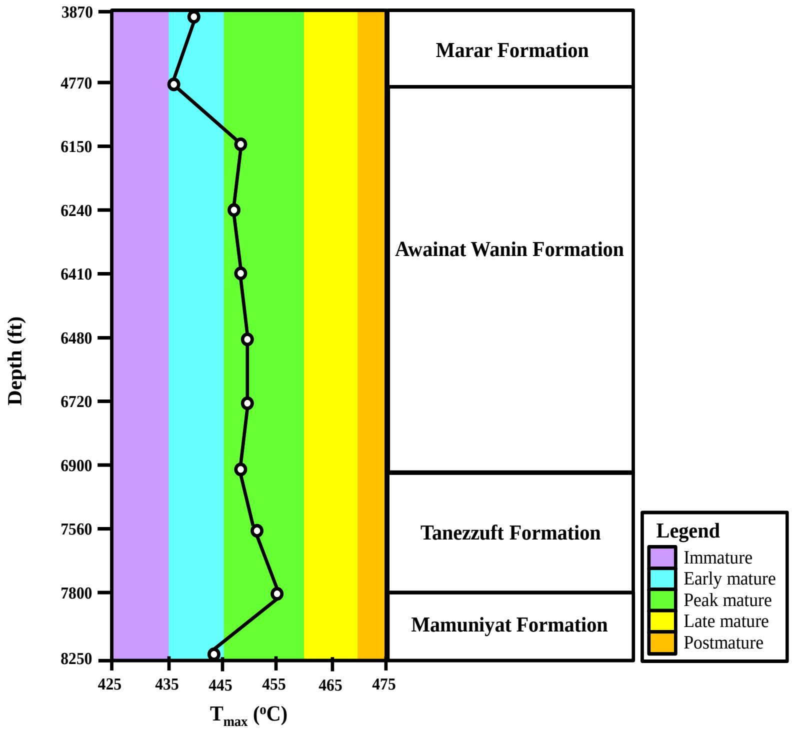

Fig. 8: Binary plot of T_{max} vs. depth showing the thermal maturity of organic matter in the Ordovician–Carboniferous shales in well A1-NC175 (fields after Peters and Cassa, 1994).

 Copyright: © 2026 by the authors. Submitted for possible open access publication under the terms and conditions of the Creative Commons Attribution (CC BY) license (https://creativecommons.org/licenses/by/4.0/).

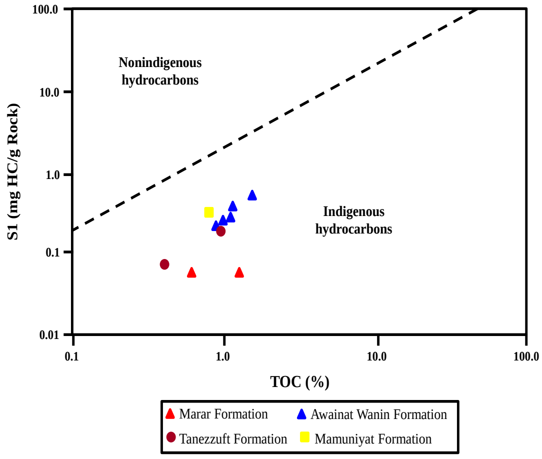

Fig. 9: Binary plot of TOC vs. S1 showing the indigeneity of hydrocarbons in the Ordovician–Carboniferous shales in well A1-NC175 (fields after Hunt, 1996).

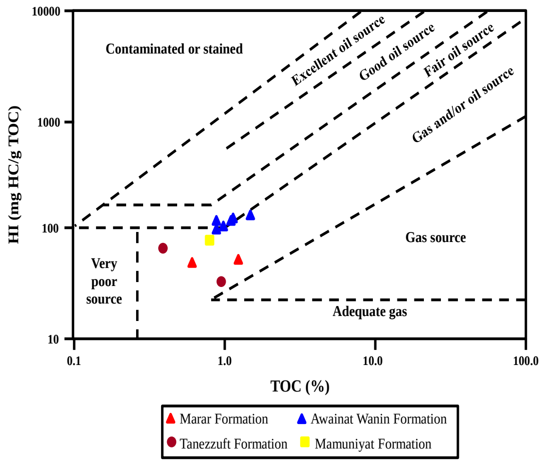

Fig. 10: Binary plot of TOC vs. HI showing the hydrocarbon potential of the Ordovician–Carboniferous shales in well A1-NC175 (fields after Jackson et al., 1985).

 Copyright: © 2026 by the authors. Submitted for possible open access publication under the terms and conditions of the Creative Commons Attribution (CC BY) license (https://creativecommons.org/licenses/by/4.0/).

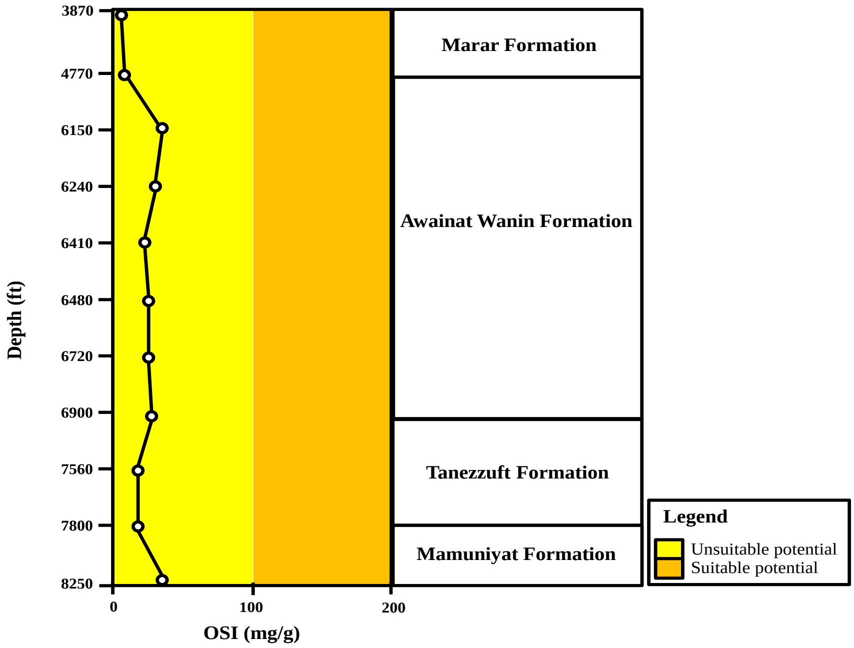

Fig. 11: Binary plot of OSI vs. depth showing the potential for recoverable shale oil from the Ordovician–Carboniferous shales in well A1-NC175 (fields after Tian et al., 2024).

Table 4: Natural gas types in the Ordovician–Carboniferous sediments in well A1-NC175

Formation	Lithology	Depth (ft)	C1	C2	C3	i-C4	n-C4	i-C5	n-C5	C6+
Dembaba	Limestone	2750	39.42	3.42	8.41	4.72	11.91	9.87	10.52	11.73
		3050	87.44	1.28	3.16	1.19	1.65	0.95	0.8	3.53
	Shale	3100	88.18	0.9	1.88	1.62	1.29	1.25	0.87	4
Assedjefar	Sandstone	3400	66.05	16.5	13.73	1.5	1.73	0.29	0.2	-
		3600	56.94	12.92	17.44	3.2	4.35	1.78	1.34	2.03
		3750	43.65	27.3	24.1	2.13	2.25	0.25	0.32	-
		3850	59.7	23.33	12.58	1.5	1.97	0.54	0.38	-
Marar	Shale	3950	51.7	24.92	16.51	2	2.72	0.92	0.74	0.49
		4000	49.63	21.8	22.94	2.03	3	0.35	0.24	-
		4050	42.03	15.52	25.2	4.79	8.73	1.73	1.29	0.71
		4200	53.17	20.35	15.34	3.43	5.56	1.07	0.72	0.36
		4350	36.71	21.49	31.66	3.12	5.37	0.85	0.57	0.23
		4450	27.08	22.89	37.94	3.33	6.17	1.07	0.81	0.71
		4550	31.59	9.8	28.7	8.66	14.74	3.08	2.15	1.28
		4750	16.34	13.82	34.54	7.92	17.09	4.35	3.46	2.48
		4850	25.56	25.52	35.89	2.8	7	1.16	1.05	1.02
		5100	29.28	23.36	29.3	2.55	8.64	2.21	2.14	2.52
		5350	31.17	16.72	29.76	3.39	11.61	2.94	2.56	1.85
		5500	24.34	19.95	31.91	3.5	11.42	3.29	2.88	2.71
		5700	24.49	15.46	24.37	4.08	14.76	5.43	5.49	5.92
		5800	23.38	13.63	21.84	5.63	13.97	7.02	6.32	8.21
Awainat Wanin	Shale	6000	21.47	19.92	25.04	4.56	12.85	4.52	5.57	6.07
		6100	17.14	20.3	30.6	5	14.88	4.05	4.82	3.2
		6250	14.94	23.4	32.97	4.62	13.38	3.59	3.94	3.16
		6450	17.4	26.26	33.51	4.16	11.22	2.7	2.67	2.08
		6700	12.62	26.25	35.56	4.26	12.59	3	3.27	2.46
Tadrart	Sandstone	7050	13.35	25.22	35.72	4.7	12.34	3.11	3.03	2.53
Tanezzuft	Shale	7400	20.48	22.25	30.14	4.79	12	3.96	3	3.36
		7750	19.83	13.59	22.7	14.68	12.76	9.2	2.87	4.37

 Copyright: © 2026 by the authors. Submitted for possible open access publication under the terms and conditions of the Creative Commons Attribution (CC BY) license (https://creativecommons.org/licenses/by/4.0/).

Table 5: Isotopic composition of gases in the Ordovician–Carboniferous sediments in well A1-NC175

Formation	Lithology	Depth (ft)	$\delta^{13}C1$	$\delta^{13}C2$	$\delta^{13}C3$	$\delta^{13}nC4$	$\delta^{13}nC5$	$\delta^{13}C_{CO2}$
Dembaba	Limestone	2750	-59.6	-27.83	-28.63	-28.32	-	-
		3050	-48.11	-	-	-	-	-
	Shale	3100	-44.22	-	-	-	-	-
		3300	-43.89	-	-	-	-	-
Assedjefar	Sandstone	3400	-50.71	-25.96	-29.57	-29.74	-	-
		3600	-45.46	-31.15	-30.09	-29.56	-	-
		3750	-44.3	-31.95	-30.24	-28.34	-	-
		3850	-43.59	-32.63	-30.5	-28.66	-	-
Marar	Shale	3950	-34.03	-29.74	-29.59	-28.6	-	-
		4000	-45.25	-32.97	-30.93	-30	-	-
		4050	-39.56	-31.85	-30.55	-29.28	-	-
		4200	-43.43	-33.02	-31.52	-29.53	-29.79	-
		4350	-45.04	-32.74	-31.84	-30.9	-30.18	-19.79
		4450	-45.29	-33.06	-31.23	-30.43	-28	-
		4550	-50.97	-32.91	-31.91	-29.55	-29.02	-
		4750	-45.28	-33.64	-32.15	-29.64	-	-
		4850	-47.78	-33.29	-32.29	-31.57	-	-18.72
		5100	-45.36	-33.8	-34.6	-32.39	-	-
		5350	-46.11	-35.3	-34.84	-32.58	-30.6	-
		5500	-44.7	-33.75	-34.44	-32.07	-30.07	-
		5700	-47.38	-34.08	-33.8	-32.23	-31.88	-
		5800	-47.3	-33.75	-31.61	-29.58	-28.19	-
Awainat Wanin	Shale	6000	-45.75	-35.36	-33.15	-31.06	-29.98	-
		6100	-45.1	-36.04	-33.31	-32	-30.22	-
		6250	-45.02	-36.4	-34.13	-30.25	-30.71	-22.06
		6450	-44.54	-35.87	-33.69	-31.4	-30.44	-22.68
		6700	-44.77	-36.28	-33.78	-31.55	-30.7	-
Tadrart	Sandstone	7050	-44.03	-37	-33.5	-	-	-
Tanezzuft	Shale	7400	-46.23	-36.55	-33.72	-31.02	-30.79	-
		7750	-41.91	-24.83	-23.16	-20.74	-20.79	-

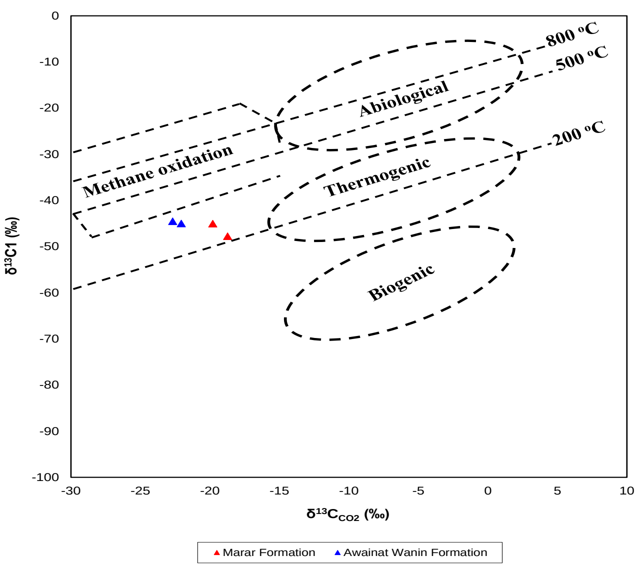

 | Copyright: © 2026 by the authors. Submitted for possible open access publication under the terms and conditions of the Creative Commons Attribution (CC BY) license (https://creativecommons.org/licenses/by/4.0/).

Fig. 12: Binary plot of $\delta^{13}C_{CO2}$ vs. $\delta^{13}C1$ showing the CO_2 origin in the Marar and Awainat Wanin formations in well A1-NC175 (fields after Cao et al., 2016).

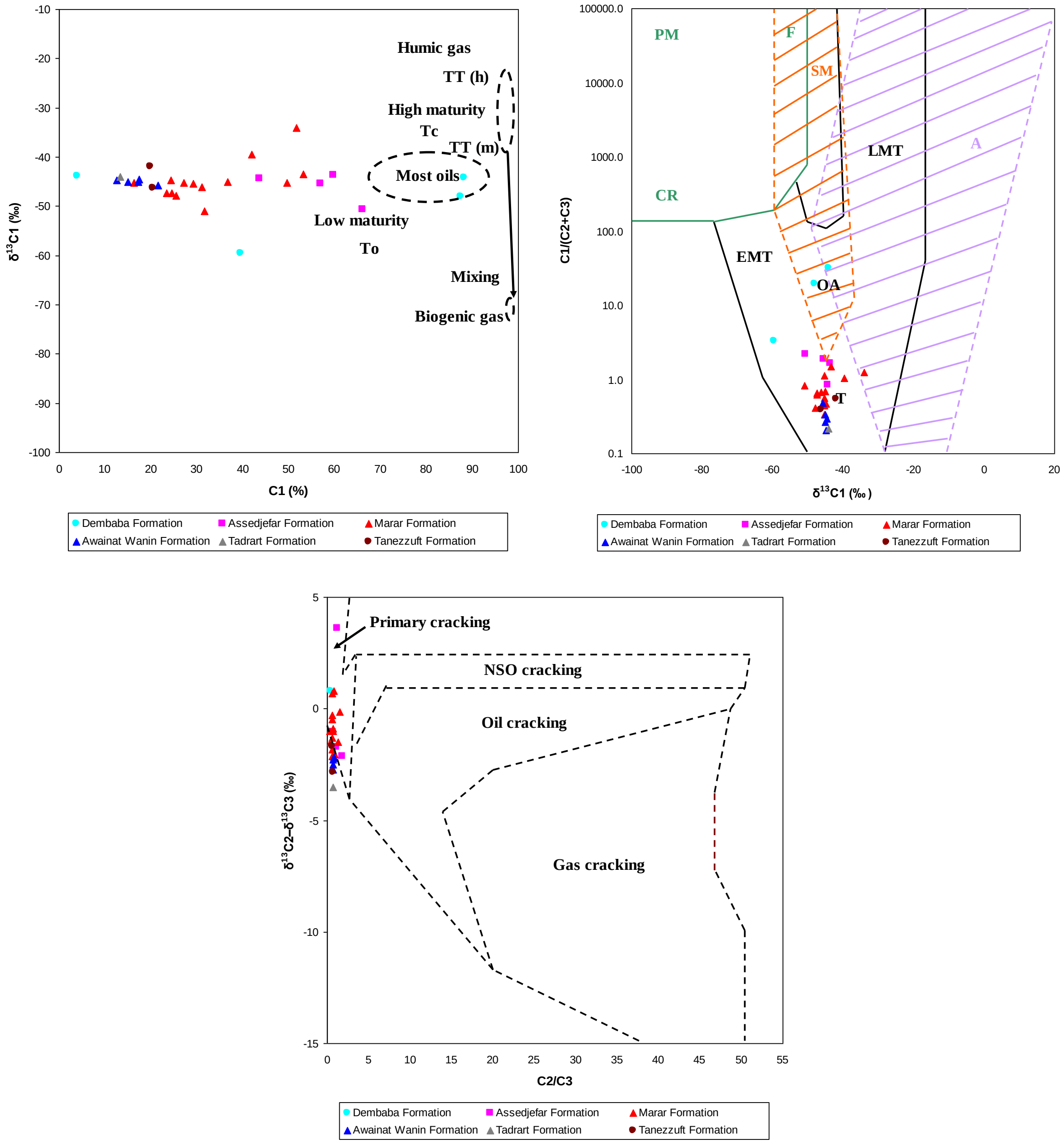

Fig. 13: Binary plots (C1 vs. $\delta^{13}C1$ (M = mixed, To = thermal oil, TT (m) = thermal marine or mixed, Tc = thermal condensate, TT (h) = thermal humic, fields after Hassanzadeh et al., 2018), $\delta^{13}C1$ vs. C1/(C2+C3) (PM = primary microbial, SM = secondary microbial, CR= CO_2 reduction, F= methyl-type fermentation, A = abiotic, T = thermogenic, EMT = early mature thermogenic gas, LMT = late mature thermogenic gas, OA = oil associated thermogenic gas, fields after Milkov and Etiope, 2018), and C2/C3 vs. $\delta^{13}C2$–$\delta^{13}C3$ (fields after Lorant et al., 1998)) showing the origin of hydrocarbon gases in the Ordovician–Carboniferous sediments in well A1-NC175.

 Copyright: © 2026 by the authors. Submitted for possible open access publication under the terms and conditions of the Creative Commons Attribution (CC BY) license (https://creativecommons.org/licenses/by/4.0/).

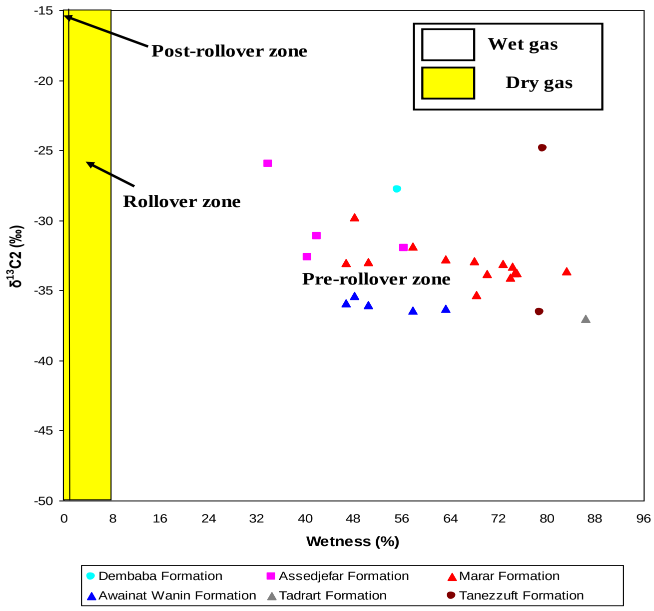

Fig. 14: Binary plot of wetness vs. $\delta^{13}C2$ showing the gas evolution in the Ordovician–Carboniferous sediments in well A1-NC175 (fields after Feng et al., 2016).

Acknowledgment

We extend our sincere thanks to the National Oil Corporation (NOC), Libya, for supplying the chemical data.

References

[1] Aboglila, S., Albaghdady, A., Farifr, E. and Alborky, A. (2020): Petroleum geochemistry regional study of Murzuq Basin: Insights from biomarkers characteristic, stable carbon isotope and environmental characterization. Petroleum and Petrochemical Engineering Journal; 4(1): 000215.

[2] Aboglila, S., Elaalem, M., Ezlit, Y. and Farifr, E. (2018): Geochemical characteristics of six formations based on organic geochemical parameters, Murzuq Basin, Libya. Advances in Research; 15(4): 1-11.

[3] Abohajar, A., Littke, R., Schwarzbauer, J., Weniger, P. and Boote, D.R.D. (2015): Biomarker characteristics of potential source rocks in the Jabal Nafusah area, NW Libya: Petroleum systems significance. Journal of Petroleum Geology; 38(2): 119-155.

[4] Albaghdady, A., Aboglila S., Farifr, E., Ramadan, M. and Alburki, A. (2020): Source Rock Characterization of Silurian Tanezzuft and Devonian Awaynat Wanin formations

 Copyright: © 2026 by the authors. Submitted for possible open access publication under the terms and conditions of the Creative Commons Attribution (CC BY) license (https://creativecommons.org/licenses/by/4.0/).

the northern edge of the Murzuq Basin, south west Libya. Petroleum and Petrochemical Engineering Journal; 4(1): 000216.

[5] Albaghday, A.A., Aboglila, S., Abdullah, M.A., Abousif, A.M.A., Farifr, E. and Targhi, M.H. (2024): Geochemical evaluation of the Silurian, Devonian, and carboniferous source rocks at the Erawin Field, Murzuq Basin, SW Libya. Journal of Scientific Research and Reports; 30(10): 465-481.

[6] Albriki, K., Guoqi, W., Wang, F., El Zaroug, R. and Abdullah, A. (2024): Shale gas play of the Silurian hot shale, Ghadames Basin, North Africa: Insights from integrated geochemistry and basin modeling. Journal of African Earth Sciences; 210: 105152.

[7] Albriki, K., Wang, F., Li, M., El Zaroug, R., Ali, A., Samba, M., Wiping, F. and Mohammed, R.S. (2022): Silurian hot shale occurrence and distribution, organofacies, thermal maturation, and petroleum generation in Ghadames Basin, North Africa. Journal of African Earth Sciences; 189: 104497.

[8] Aziz, A. (2000): Stratigraphy and hydrocarbon potential of the Lower Palaeozoic succession of License NC-115, Murzuq Basin, SW Libya. In: M.A. Sola, and D. Worsley (Eds) Geological Exploration in Murzuq Basin. Elsevier, Amsterdam; pp. 349-368.

[9] Belaid, A., Krooss, B.M. and Littke, R. (2010): Thermal history and source rock characterization of a Paleozoic section in the Awbari Trough, Murzuq Basin, SW Libya. Marine and Petroleum Geology; 27(3): 612-632.

[10] Boshnyif, A., Shaltami, O.R., Belhaj. A. and Ben Hkoma, M. (2025): Organic geochemistry of the Hot Shale Member of the Tanezzuft Formation of wells B1-23 and Q1-23, Ghadames Basin, NW Libya with regional correlation. Alqalam Journal of Medical and Applied Sciences (AJMAS); 8(1): 277-291.

[11] Cao, C., Lv, Z., Li, L. and Du, L. (2016): Geochemical characteristics and implications of shale gas from the Longmaxi Formation, Sichuan Basin, China. Journal of Natural Gas Geoscience; 1: 131-138.

[12] Carr, I.D. (2002): Second-order sequence stratigraphy of the Palaeozoic of North Africa. Journal of Petroleum Geology; 25: 259-280.

[13] Dembicki, H.J. (2009): Three common source rock evaluation errors made by geologists during prospect or play appraisals. American Association of Petroleum Geologists Bulletin; 93(3): 341-356.

 Copyright: © 2026 by the authors. Submitted for possible open access publication under the terms and conditions of the Creative Commons Attribution (CC BY) license (https://creativecommons.org/licenses/by/4.0/).

[14] Edegbai, A.J. and Ogbe, O.B. (2024): Geological and geochemical evaluation of shale gas potential of the Tanezzuft Formation, Ghadames Basin, North Africa. Petroleum and Coal; 66(3): 842-856.

[15] EIA (U.S. Energy Information Administration, 2015): Technically recoverable shale oil and shale gas resources: Libya. Technical Report; 26p.

[16] El Diasty, W.S., El Beialy, S.Y., Anwari, T.A., Peters, K.E. and Batten, D.J. (2017): Organic geochemistry of the Silurian Tanezzuft Formation and crude oils, NC115 concession, Murzuq Basin, southwest Libya. Marine and Petroleum Geology; 86: 367-385.

[17] Elkelani, M.M.A. (2014): Silurian and Devonian source rocks and crude oils from the western part of Libya: Organic geochemistry, palynology and carbon isotope stratigraphy. Utrecht Studies in Earth Sciences; 71(42): 1-189.

[18] Fello, N., Lüning, S., Štorch, P. and Redfern, J. (2006): Identification of early Llandovery (Silurian) anoxic palaeo-depressions at the western margin of the Murzuq Basin (southwest Libya), based on gamma-ray spectrometry in surface exposures. GeoArabia; 11(3): 101-118.

[19] Feng, Z.Q., Liu, D., Huang, S.P., Wu, W., Dong, D.Z., Peng, W.L. and Han, E.X. (2016): Carbon isotopic composition of shale gas in the Silurian Longmaxi Formation of the Changning area, Sichuan Basin. Petroleum Exploration and Development; 43(5): 769-777.

[20] Galeazzi, S., Point, O., Haddadi, N., Mather and Druesne, D. (2010): Regional geology and petroleum systems of the Illizi-Berkine area of the Algerian Saharan Platform: An overview. Marine and Petroleum Geology; 27: 143-178.

[21] Hall, L.S., Boreham, C.J., Edwards, D.S., Palu, T.J., Buckler, T., Hill, A.J. and Troup, A. (2016): Cooper Basin source rock geochemistry: Regional hydrocarbon prospectivity of the Cooper Basin. Geoscience Australia, Part2; 62p.

[22] Hall, P.B., Bjoroy, M., Ferriday, I.L. and Ismail, Y. (2010): Libyan Murzuq Basin source rocks. American Association of Petroleum Geologists (AAPG) Search and Discovery Article #10271; 24p.

[23] Hallett, D. (2002): Petroleum geology of Libya. Amsterdam, Elsevier Inc., 503p.

[24] Hallett, D. and Clark-Lowes, D. (2016): Petroleum geology of Libya. 2nd edition, Amsterdam, Elsevier Inc., 404p.

 | Copyright: © 2026 by the authors. Submitted for possible open access publication under the terms and conditions of the Creative Commons Attribution (CC BY) license (https://creativecommons.org/licenses/by/4.0/).

[25] Haq, B.U. and Schutter, S.R. (2008): A chronology of Palaeozoic sea-level changes. Science; 322: 64-68.

[26] Hassanzadeh, P., Rabbani, A.R., Hezarkhani, A. and Khajooie, S. (2018): Assessing lateral continuity within the Yammama Reservoir in the Foroozan Oilfield, Offshore Iran: An integrated study. Acta Geologica Sinica; 92(6): 2405-2415.

[27] Hodairi, T. and Philp, P. (2011): Geochemical investigation of Tanezzuft Formation, Murzuq Basin, Libya. AAPG Search and Discovery Article #10344; 22p.

[28] Hrouda, M. (2004): The hydrocarbon source potential of the Palaeozoic rocks of the Ghadames Basin, NW Libya. Unpublished PhD Thesis, University of Newcastle, UK.

[29] Hunt, J.M. (1996): Petroleum geochemistry and geology. 2nd edition, W. H. Freeman; 743p.

[30] Jackson, K.S., Hawkins, P.J. and Bennett, A.J.R. (1985): Regional facies and geochemical evaluation of southern Denison Trough. Journal of Australian Petroleum Production and Exploration; 20: 143-158.

[31] Jones, R.W. (1987): Organic facies. In: Brooks, J., Welte D. (Eds.), Advances in Petroleum Geochemistry 2. Academic Press, London; pp. 1-90.

[32] Longford, F.F. and Blanc-Valleron, M.M. (1990): Interpreting Rock–Eval pyrolysis data using graphs of pyrolyzable hydrocarbons vs. total organic carbon. American Association of Petroleum Geologists Bulletin; 74: 799-804.

[33] Lorant, F., Prinzhofer, A., Behar, F. and Huc, A.Y. (1998): Carbon isotopic and molecular constraints on the formation and the expulsion of thermogenic hydrocarbon gases. Chemical Geology; 147(3-4): 249-264.

[34] Lüning, S., Craig, J., Loydell, D.K., Storch, P. and Fitches, B. (2000): Lower Silurian "hot shales" in North Africa and Arabia: Regional distribution and depositional model. Earth -Science Reviews; 49: 121-200.

[35] McDougall, N., Quin, J.G. Vila Pont, J. and Tawengi, K. (2005): Sedimentology, sequence stratigraphy and large-scale architecture of the Upper Ordovician Mamuniyat and Melaz Shugran Formations based on outcrop studies of the Gargaf area. Repsol Exploration Libya Finding Team, Madrid. Confidential REPSOL Report; 95p.

[36] Meinhold, G., Howard, J., Abutarruma, Y., Thusu, B. and Whitham, A.G. (2021): Mineralogical and geochemical changes in subsurface shales straddling the

 Copyright: © 2026 by the authors. Submitted for possible open access publication under the terms and conditions of the Creative Commons Attribution (CC BY) license (https://creativecommons.org/licenses/by/4.0/).

Ordovician–Silurian boundary in the eastern Kufra Basin, Libya. Journal of African Earth Sciences; 184: 104378.

[37] Meinhold, G., Le Heron, D.P., Elgadry, M. and Abutarruma, Y. (2016): The search for ‘hot shales’ in the western Kufra Basin, Libya: Geochemical and mineralogical characterisation of outcrops, and insights into latest Ordovician climate. Arabian Journal of Geosciences; 9(62).

[38] Milkov, A.V. and Etiope, G. (2018): Revised genetic diagrams for natural gases based on a global dataset of> 20,000 samples. Organic Geochemistry; 125: 109-120.

[39] Muhammed, F.K. (2024): Shale oil geochemistry: A case study of the Assedjefar Formation in well A1-N C115, El Sharara Field, Murzuq Basin, SW Libya. Unpublished MSc Thesis, Benghazi University, Libya.

[40] Musa, M.O. (2019): Thermal maturity and time of oil generation of the source rock, Murzuq Basin. Albayan Scientific Journal; 4: 194-206.

[41] Peters, K.E. and Cassa, M.R. (1994): Applied source rock geochemistry. In: Magoon, L.B., Dow, W.G. (Eds.): The petroleum system from source to trap, American Association of Petroleum Geologists (AAPG) Memoir; 60: 93-117.

[42] Reed, S. and Ewan, H.M. (1986): Geochemical report. Norse Hydro A/S, 6407/7-1, (available at https://www.npd.no/%20engelsk/cwi/pbl/geochemical_pdfs/474_7.pdf).

[43] Shalbak, F.A. (2015): Palaeozoic petroleum systems of the Murzuq Basin, Libya. Unpublished PhD Thesis, Barcelona University, Spain.

[44] Shaltami, O.R. (2024): Elemental geochemistry of the Awainat Wanin Formation in three selected areas, Murzuq Basin, SW Libya. Global Scientific Journals (GSJ); 12(2): 992-1016.

[45] Shaltami, O.R., Algomati, A.E., Sharma, S. and Afkareen, M. (2025): Elemental geochemistry of source rocks and reservoirs in Libya: A case study of the Tanezzuft, Lower Akakus, and Sirte formations. Libyan Journal of Engineering Science and Technology (LJEST); 5(3): 251-259.

[46] Shaltami, O.R., Bustany, I., Fares, F.F, Errishi, H. and EL Oshebi, F.M. (2021): Unconventional hydrocarbons in the Hot Shale Member of the Tanezzuft Formation. 1st edition, Amazon Kindle Direct Publishing (KDP); 123p.

[47] Tian, H., Wu, H., Yan, W., Feng, Z., Li, C., Ren, L. and Xu, H. (2024): Evaluation method of oil saturation index OSI for shale oil reservoir based on well logging data. Frontiers in Earth Science; 12: 1358268.

 Copyright: © 2026 by the authors. Submitted for possible open access publication under the terms and conditions of the Creative Commons Attribution (CC BY) license (https://creativecommons.org/licenses/by/4.0/).

[48] Tissot, B.P. and Welte, D.H. (1984): Petroleum formation and occurrence. 2nd edition. Springer Berlin, Heidelberg; 702p.

[49] Vos, R.G. (1981): Deltaic sedimentation in Devonian of Western Libya. Sedimentary Geology; 29: 67-88.

[50] Whiticar, M.J. (1999): Carbon and hydrogen isotope systematic of microbial formation and oxidation of methane. Chemical Geology; 161: 291-314.

Disclaimer/Publisher's Note: The statements, opinions, and data contained in all publications are solely those of the individual author(s) and contributor(s) and not of **AJHAS** and/or the editor(s). **AJHAS** and/or the editor(s) disclaim responsibility for any injury to people or property resulting from any ideas, methods, instructions, or products referred to in the content.

 Copyright: © 2026 by the authors. Submitted for possible open access publication under the terms and conditions of the Creative Commons Attribution (CC BY) license (https://creativecommons.org/licenses/by/4.0/).